International Journal of Pharmaceutics 411 (2011) 27–35

Contents lists available at ScienceDirect

International Journal of Pharmaceutics

journal homepage: www.elsevier.com/locate/ijpharm

Fast assessment of the surface distribution of API and excipients in tablets using NIR-hyperspectral imaging

Felicidad Franch-Lage[a], José Manuel Amigo[b,*], Erik Skibsted[c], Santiago Maspoch[a], Jordi Coello[a]

[a] Departament de Química, Unitat de Química Analítica, Universitat Autònoma de Barcelona, Spain
[b] Department of Food Science, Quality and Technology, Faculty of Life Science, University of Copenhagen, DK-1958 Copenhagen, Denmark
[c] Novo Nordisk A/S, Maaloev, Denmark

ARTICLE INFO

Article history:
Received 21 December 2010
Received in revised form 8 March 2011
Accepted 9 March 2011
Available online 16 March 2011

Keywords:
NIR
Hyperspectral imaging
Tablets
Lorazepam
MCR
Multivariate curve resolution
Content uniformity

ABSTRACT

The inclusion of hyperspectral imaging systems in the manufacturing and development of pharmaceutical products is allowing a successful improvement in the quality control of solid dosage forms. The correct distribution not only of active pharmaceutical ingredient (API) but also of the rest of excipients is essential to assure the correct behavior of the tablet when ingested. This is especially relevant in tablets with low content of potent APIs, in which the prescribed intake dosage frequently corresponds to half-a-tablet. Therefore, the aim of this work is to study the surface distribution of the compounds in tablets with low API content. The proposed procedure includes the scanning of the tablet surface using near infrared hyperspectral spectroscopy in association with multivariate curve resolution (MCR) techniques to obtain selective pictures for each individual compound and to allow the fast assessment of their distribution in the measured surface.

As an example, a set of commercial Lorazepam tablets (approximately 1% mass fraction of API, and four excipients) were analyzed. The results obtained show the capacity of the proposed methodology as an expedite approach to evaluate the uniformity of the contents between and within tablets. A method to estimate the homogeneity distribution of API in the two halves of the tablet is also proposed.

1. Introduction

Pharmaceutical industries invest considerable amounts of time and money in developing and verifying methods to assure the final quality of solid dosage forms (SDFs) (Amigo, 2010a), mainly determined by both the distribution and composition of the internal and external matrices. The internal matrix is formed by the active pharmaceutical ingredient (API) and the excipients, being the distribution of its components in this solid mixture responsible for tablet behavior in different stages like compaction and release in the human body. These components should be distributed in the tablets as homogeneously as possible. If the API agglomerates in prior steps of the production process (blending, granulation, etc.), significant differences would occur between tablets. But even in the case of a uniform batch, a certain degree of agglomeration or segregation (i.e. non-uniform distribution) in a given tablet may happen. As stated above, this fact can affect several important parameters. However, it is especially important in the case of SDFs, in which the therapeutical dose is a fraction of the tablet. A non-uniform distribution of API means that the actual dose ingested by the patient would not be the same in the different fractions, which can be particularly critical if the API has a low mass proportion.

Recently, the European Medicines Agency (EMeA) adopted a revision of the "*Guideline on Summary of Product Characteristics*" which states that in case of tablets designed with a score line (Fig. 1, right), information should be given whether or not a reproducible division of the tablets has been shown (e.g. "the score line is only to facilitate breaking for ease of swallowing and not to divide into equal doses" or "the tablet can be divided into equal halves") (E.C.E.a.I.D.-G.E., 2005).

Usual analytical quality control in divisible dosages consists in determining the API content in both halves of the tablets by a standard technique such as high performance liquid chromatography (HPLC), which is destructive and time consuming. Furthermore, it relies on the ability of the analyst to divide the tablet and offers no information about the distribution of the components.

Abbreviations: API, active pharmaceutical ingredient; CMS, sodium-carboxymethyl starch; CV(%), coefficient of variation; EMeA, European Medicines Agency; FT-NIR, Fourier transform-near infrared; HPLC, high performance liquid chromatography; LAC, lactose monohydrate; MCC, microcrystalline cellulose; MCR, multivariate curve resolution; MCT, mercury cadmium telluride detector array; MgSt, magnesium stearate; mid-IR, middle infrared; NIR, near infrared; SDBP, standard deviation between pixels; SDF, solid dosage form; SNV, standard normal variate; US-FDA, United States Food and Drugs Administration; %LOF, percentage of lack of fit.

* Corresponding author. Tel.: +34 667504477.
E-mail address: jmar@life.ku.dk (J.M. Amigo).

0378-5173/$ – see front matter © 2011 Elsevier B.V. All rights reserved.
doi:10.1016/j.ijpharm.2011.03.012

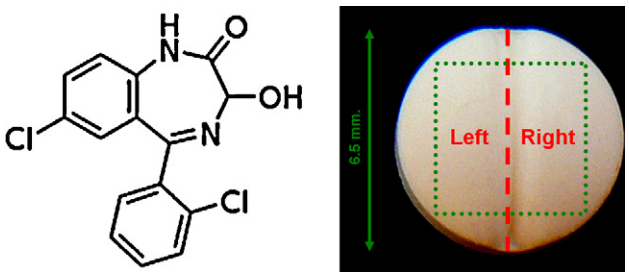

Fig. 1. Lorazepam chemical structure (left) and Lorazepam® commercial tablet (right). The green dotted square indicates the area measured in each tablet; the red dashed line refers to the division of the measured area following the score of the tablet. (For interpretation of the references to color in this figure legend, the reader is referred to the web version of the article.)

Hyperspectral imaging is being introduced in pharmaceutical research laboratories to overcome the abovementioned drawbacks of classical techniques (Amigo, 2010a; Chan et al., 2005; Gendrin et al., 2008; Lewis et al., 2001; Reich, 2005; Roggo et al., 2005), providing information about the surface distribution of the ingredients from one slice of the tablet. Among others, vibrational spectroscopic imaging techniques, as middle-infrared (mid-IR), near infrared (NIR), and Raman imaging are the most used and relevant ones (Amigo, 2010a). Their use will depend on the final target pursued, being out of the scope of this paper to make a comparison between them. Nevertheless, the readers are encouraged to look for the supplied references.

The main benefit from hyperspectral devices is the obtaining one whole spectral pattern in each pixel of the measured surface. The final result of the measurement is a three dimensional data structure or a hyperspectral data cube (Fig. 2). This structure can also be visualized as a three-dimensional array **D** of dimensions ($X \times Y \times \lambda$) in which each pixel ($X$–$Y$ coordinate) contains a spectrum of λ wavelengths. The attractiveness of obtaining surface information together with the proper data analysis methods allowed new research fields in pharmaceutics (Amigo et al., 2009; Gendrin et al., 2008; Ravn et al., 2008; Roggo et al., 2005), providing the perfect foundations to obtain reliable and accurate information of the correct distribution of components in tablets.

As mentioned above, the main advantage of Chemical Imaging techniques relies in the amount of information obtained for each single sample. Therefore, the use of multivariate data analysis methods to extract the desired information (i.e. distribution maps for each individual component of the tablet) is mandatory (Amigo, 2010a; Amigo et al., 2008; Amigo and Ravn, 2009). In this context, several regression and resolution methods have been previously tested to obtain quantitative and selective information on the distribution of the components in each pixel (Amigo and Ravn, 2009; Ravn et al., 2008). One of the methods with increasing importance in CI techniques is the augmented version of multivariate curve resolution (MCR) (Amigo and Ravn, 2009; Cruz et al., 2009; de Juan et al., 2004, 2009). It allows the decomposition of the original data cube into two sub-matrices, including concentration surfaces for each component and spectral information.

Lorazepam (Fig. 1, left) is one of the most commonly prescribed antidepressant drugs due to its quick response in treating fast onset panic anxiety (Lader, 1984). This drug has strong sedative and hypnotic effects and the duration of clinical effects from a single dose makes it an appropriate choice for the short-term treatment of insomnia, particularly in the presence of severe anxiety. Due to its effects and proneness to generate addiction, the United States Food and Drugs Administration (US-FDA) advises against its usage (Chen et al., 2009).

In general, tablets containing Lorazepam have a small size (e.g. those used in this work had 6.5 mm diameter approximately) and a low concentration (in mass fraction) of API in a mixture of several excipients. The tablets used in this study (see further sections) contain four excipients. Microcrystalline cellulose (MCC) and lactose monohydrate (LAC) are part of a class named binders and fillers (Aulton, 2007). Their role is to create a powder mixture that has good flow and compressibility properties. Another excipient in the tablets is magnesium stearate (MgSt). This is a lubricant which provides anti-sticking properties during the tabletting process (Rowe et al., 2006). For instance, poor distribution of the lubricant particles may be the root of hardness or dissolution problems in the tablets. The last excipient is sodium-carboxymethyl starch (CMS), a cellulose derivative part of the disintegrants class, which promotes expansion and dissolution when wet, thereby causing tablet disintegration. For these reasons, it is essential to assess the cor-

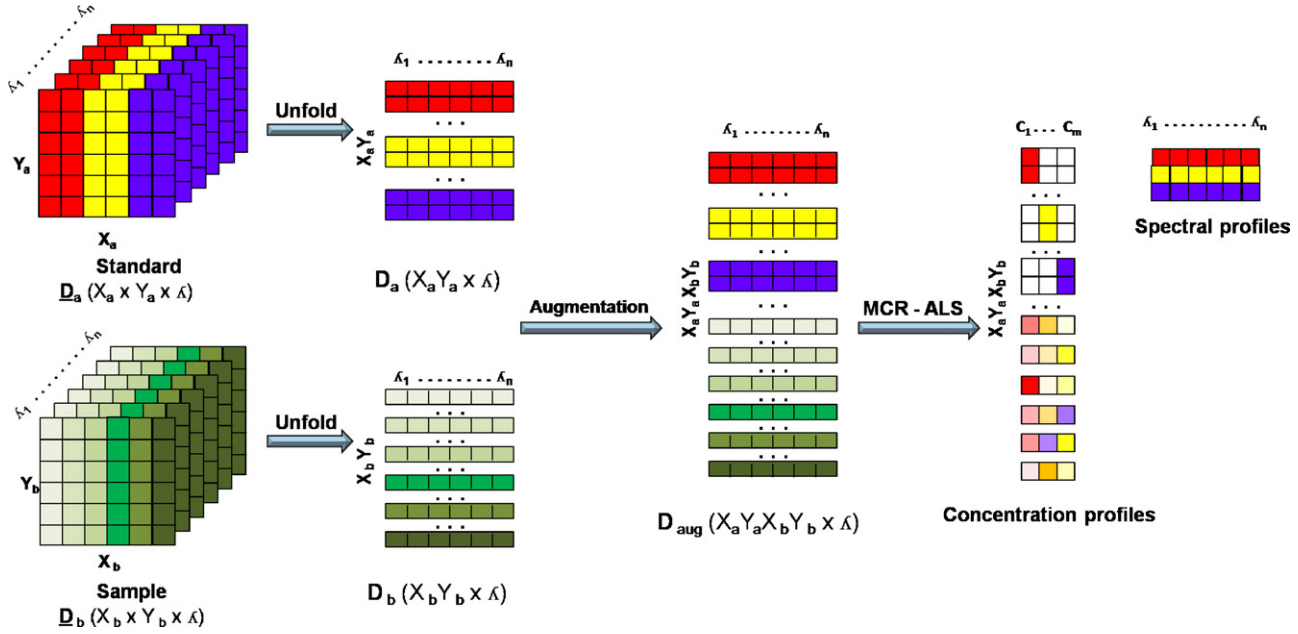

Fig. 2. MCR with image augmentation. The example assumes the existence of three compounds (red, yellow and purple). (For interpretation of the references to color in this figure legend, the reader is referred to the web version of the article.)

rect distribution not only of the API but also of the remaining excipients.

Hence, this work presents the development of a robust, fast and reliable methodology to study the signal contribution (in percentage) of each compound in the Lorazepam tablets as well as the assessment of their correct distribution in the surface to allow the quality control of the final tablet. Since the traditional methodologies for the investment of drug distribution (e.g. HPLC) are time consuming and usually require specific analytical method for each component in the tablet, the proposed methodology, joining hyperspectral image analysis and multivariate analysis (by means of MCR technique), may be a good and fast way of analyzing tablets routinely.

2. Experimental

2.1. Samples and reference compounds

Twelve tablets of Lorazepam Normon 1 mg EFG (non-coated tablets from Laboratorios Normon S.A., Madrid, Spain) were randomly selected from the same batch (a pack of 50 tablets). Pure Lorazepam was purchased from Sigma-Aldrich (St. Louis, MO, USA). The excipients for the tablet formulation were microcrystalline cellulose–MCC – from Pharma (Germany), lactose monohydrate–LAC – from Meggle (Wasserburg, Germany), magnesium sterarate–MgSt – from Peter Greven Fett-Chemie (Bad Münstereifel, Germany) and sodium carboxymethyl starch–CMS – from Pharma (Germany).

Pure compound reference tablets of the five components (Lorazepam and 4 excipients) were produced by compressing 250 mg of each into 8 mm diameter wafers on a hydraulic tablet press using 10 kN pressure during 10 s. The standard sample used for augmentation in MCR was obtained by sectioning a representative area of 15 square pixels of each pure component image.

2.2. Image acquisition

Lorazepam and pure tablets were glued onto a microscope slide, the former being previously microtomed with a Leica EM Trim (Wetzlar, Germany) equipped with a microscope. Samples were placed in such a way that the score line of the tablet was situated in the central part of the scanned surface and in a vertical position with respect to the detector. The depth of the cut was indicated by the depth of the score of the tablet. Therefore, the surface measure was close to the half of the tablet. This is the area of the tablet in which higher homogeneity distribution can be expected. The hyperspectral scanning was performed using a NIR line mapping system (Spectrum Spotlight 350 FT-NIR Microscope from PerkinElmer, Cambridge, UK) from which 8 spectral scans were co-added in each acquisition from a linear MCT detector array. An area of approximately 4 mm × 4 mm was analyzed with a spatial resolution of 25 μm per pixel. Each spectrum was measured in the near infrared 7800–4000 cm^{-1} wave number region with 16 cm^{-1} spectral resolution.

2.3. Data analysis and assessment of the final results

2.3.1. Pre-processing

After conversion of the reflectance values obtained for each image into absorbance, spectra were pre-processed to eliminate/minimize artifacts coming from the measurement (e.g. baseline drift in NIR spectra due to light scattering (Amigo, 2010a)). Hence, standard normal variate (SNV) and Savitzky–Golay smoothing (second order polynomial filter and 5 points window size) were applied to samples and standards.

2.3.2. Augmented MCR performance

Multivariate curve resolution (MCR) in its augmented version has been previously applied in hyperspectral imaging. A brief explanation is given below and further information can be obtained elsewhere (Amigo et al., 2008; de Juan et al., 2004, 2009).

This technique decomposes the unfolded image $\mathbf{D}$ ($XY \times \lambda$) into the product of two matrices. $\mathbf{C}$ ($XY \times F$) matrix contains the matricized concentration images (signal contribution); whereas $\mathbf{S^T}$ ($F \times \lambda$) contains the spectral profiles for each F component (Eq. (1)):

$$\mathbf{D} = \mathbf{CS^T} + \mathbf{E} \tag{1}$$

where $\mathbf{E}$ ($XY \times \lambda$) accounts for the experimental error. MCR works by iteratively optimizing the matrices $\mathbf{C}$ and $\mathbf{S^T}$. Thus, if the proper constraints are applied (de Juan and Tauler, 2006) (see Section 2.3.3), the result is not constrained to the pure spectra, allowing MCR to cope with minor sources of variability that may exist in the tablet (Amigo and Ravn, 2009).

The main disadvantage of MCR in Chemical Imaging is that in order to obtain good results, the studied surface must contain enough information for each component to account for the variability of the concentration in the sample (Amigo, 2010a; Amigo et al., 2008). This issue is especially relevant in samples with low concentrations of chemical compounds. Augmenting the original sample with more images, a method proposed by de Juan et al. (2004), is a feasible alternative to overcome this problem (Amigo and Ravn, 2009; de Juan et al., 2004). This method analyses several samples simultaneously, collecting the information from one to the other (de Juan and Tauler, 2006). The main feature of the matrix augmentation is that the unfolded target sample ($\mathbf{D}_b$) is amplified with an image without selectivity problems (standard image, $\mathbf{D}_a$) in a column-wise fashion (Fig. 2):

This "standard" image is composed by sections of each pure component of the tablet (Fig. 2). It can be easily generated with images of the pure compounds. Working with this standard sample, much more accurate information is submitted to MCR at the same time, since experimental variability (instrumental noise) is also reflected in the augmented image, allowing MCR to get hold of selective information in the iterations (Eq. (2)):

$$\begin{bmatrix} \mathbf{D}_a \\ \mathbf{D}_b \end{bmatrix} = \begin{bmatrix} \mathbf{C}_a \\ \mathbf{C}_b \end{bmatrix}^{\mathbf{S^T}} + \begin{bmatrix} \mathbf{E}_a \\ \mathbf{E}_b \end{bmatrix} \tag{2}$$

where $\mathbf{C}_a$ and $\mathbf{C}_b$ contain the concentration profiles for the standard image (a) and the sample (b) for each F compound. When the concentration profiles obtained are refolded to the original shape, distribution maps for each component are reached. Moreover, the similarity (in terms of correlation) between the obtained spectral profiles ($\mathbf{S^T}$) and the pure spectra of the compunds are a key factor to evaluate the model.

An important implication of using pure component spectra in MCR is that the concentrations of the chemical images vary from approximately zero to one since the pure component spectra are arbitrarily set to concentration one. The MCR prediction values for a component are thus fractions or percentages of the pure component sample, which however only approximates the mean percentage of the component in the actual sample (Ravn, 2009). As de Juan et al. (2009) pointed out, the association of concentration maps obtained by MCR should be more correctly described as the signal contribution of a certain constituent to the overall signals. Therefore, the concentration maps obtained should not be straightforwardly associated with compound concentrations, given the different absortivity and scattering of the compunds in the image (de Juan et al., 2009). The final signal contribution percentage of the different compounds in the image to the overall signal

measured can be easily calculated by Eq. (3):

$$\mathbf{c}'_{bi}(\%) = \frac{\sum \mathbf{c}_{bi}\mathbf{s}_i^{\mathbf{T}}}{\sum \mathbf{C}_b\mathbf{s}^{\mathbf{T}}} \times 100 \quad (3)$$

where $\mathbf{c}_{bi}$ and $\mathbf{s}_i^{\mathbf{T}}$ are the concentration and spectral profile obtained for compound i in the sample ($\mathbf{D}_b$), respectively.

2.3.3. Models application and validation of the results

Savitzky–Golay smoothing and SNV methods were implemented in in-house routines working under MATLAB v. 7.5 (The Matworks, Massachusetts, USA) and freely available upon request. For augmented MCR application, a software provided by Tauler's group was used (Jaumot et al., 2005; http://www.mcrals.info/ – accessed December 2010).

For augmented MCR analysis, non-negativity and closure constraints were imposed to the concentration profiles. No constraints were applied to the spectra because they were pre-processed using SNV. Pure spectra of the five compounds were used as initial estimations. The percentage of lack of fit (%LOF) between the obtained results and the original data measures the fit quality (de Juan and Tauler, 2006). Another parameter used to validate the calculated models with augmented MCR was the similarity (correlation coefficient) between the spectral profiles obtained and the pure spectra.

To evaluate the distribution of the concentrations obtained for each compound in each tablet, histograms of the concentration surfaces were studied and the standard deviation between pixels ($SDBP_i$) for each compound calculated (Amigo and Ravn, 2009; Furukawa et al., 2007; Jovanovic et al., 2006) (Eq. (4)):

$$SDBP_i = \sqrt{\frac{\sum_{x=1}^{X}\sum_{y=1}^{Y}\left(\hat{c}'_{ixy} - \bar{c}'_{ixy}\right)}{XY - 1}} \quad (4)$$

where $\hat{c}'_{ixy}$ accounts for the calculated concentration for each ith compound in each xyth pixel, $\bar{c}'_{ixy}$ represents the mean value of the concentration obtained for each analyte and XY is the total number of pixels.

2.3.4. Distribution in different parts of the tablet

After obtaining the concentration maps for each compound in each tablet, the values gathered in both parts of the measured surface were compared (accordingly to the position of the score line of the tablet, see Fig. 1). The surface of each tablet was scanned placing the score line a vertical position with the detector. Thus, it is possible to calculate the differences (%) in the distribution of the compounds in each half of the tablet (see Fig. 1 for the divisions made to the tablet surface), using Eq. (5):

$$(\%\text{Distribution})_{\text{left}} = \frac{\left(\hat{c}'_{bi}(\%)\right)_{\text{left}}}{2 * \left(\hat{c}'_{bi}(\%)\right)_{\text{TOTAL}}} \times 100 \quad (5)$$

The distribution for the right part is calculated the same way. Ideally, both parts should contain 50% of the contribution of each compound.

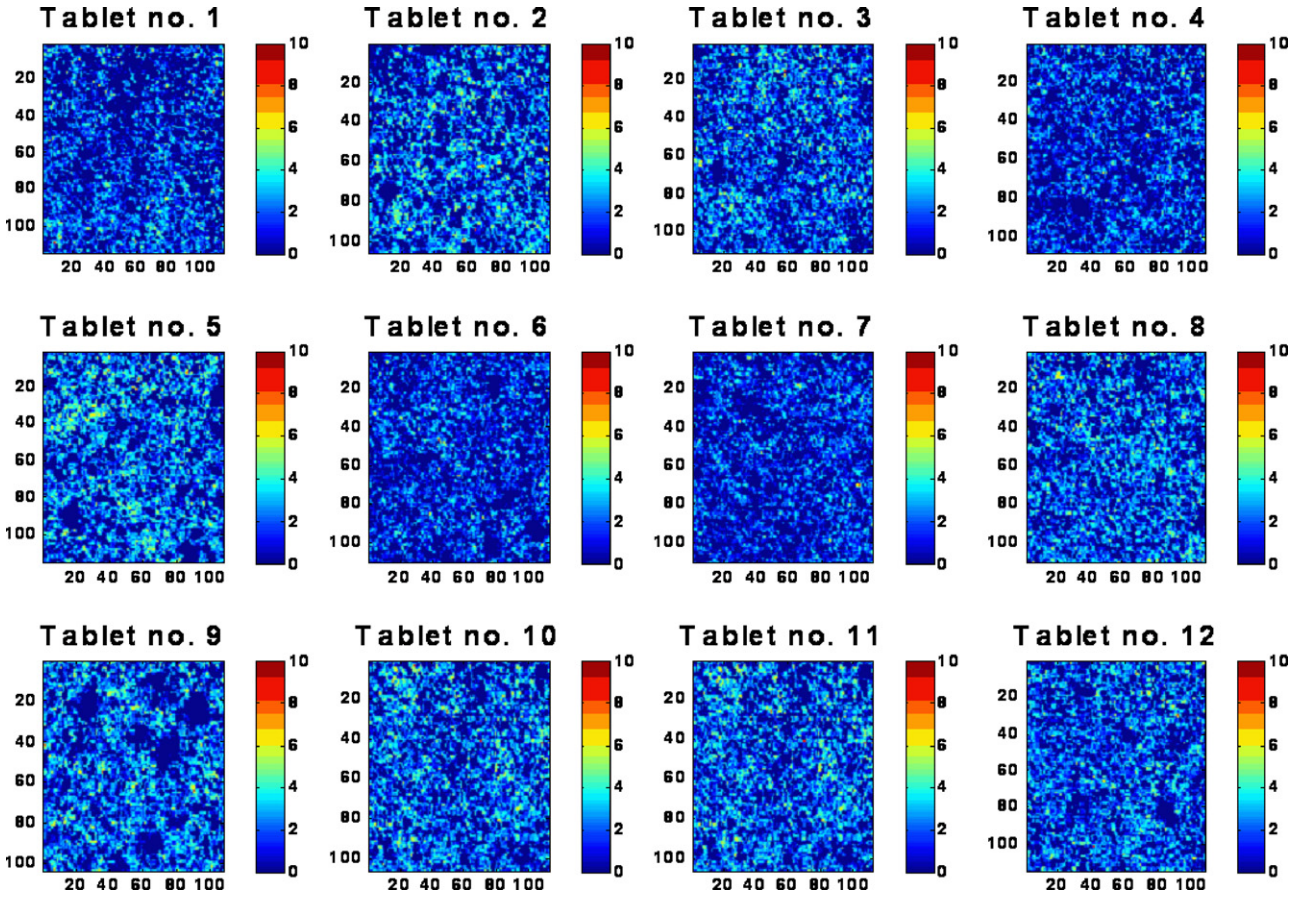

Fig. 3. Concentration maps for Lorazepam in the 12 tablets analyzed. The color scale indicates the percentage of Lorazepam in each pixel of the scanned surface.

Table 1
Mean signal contributions (in terms of percentage) and similarity coefficients calculated for each compound (standard deviation between brackets).

	Lorazepam	CMS	MgSt	MCC	LAC
Mean[a]	1.45 (0.24)	1.39 (0.20)	1.39 (0.14)	4.97 (0.90)	90.77 (0.97)
CV (%)[b]	16.60	14.06	10.15	18.05	1.07
Similarity[c]	0.99997 (0.00002)	0.99990 (0.00007)	0.99923 (0.00047)	0.99871 (0.00088)	0.94306 (0.02370)

[a] Theoretical mass fraction of Lorazepam was ≈1 wt%.
[b] Coefficient of variation calculated as $s * 100/\text{Mean}$.
[c] Correlation coefficient between the obtained spectral profiles and the pure spectrum for each analyte. Standard deviation of the 12 models between brackets.

3. Results and discussion

3.1. Lorazepam distribution

The percentages of Lorazepam obtained for the twelve tablets in each pixel of the scanned surface by using augmented MCR (re-folded concentration profile for each compound as indicated in Fig. 2) are shown in Fig. 3. At first sight, neither the presence of aggregates nor agglomeration of Lorazepam was observed, which revealed a correct distribution of Lorazepam in the surface of the tablet measured, enhancing the correct dissemination and thus heading towards a homogeneous distribution. The mean signal concentration values for Lorazepam (Table 1) were close to the nominal concentration in the tablet (≈1 wt%, according to the manufacturer). However, this comparison is not trivial since the contribution is probably related to the volume fraction more closely than to the mass fraction. The variation between tablets (measured with the standard deviation and the coefficient of variation) was within acceptable limits, allowing the correct matching between the nominal concentration and the concentration obtained with augmented MCR models.

The histograms for Lorazepam signal contribution are depicted in black in Fig. 4. As can be observed, similar pixel concentration distributions were observed for all the tablets. This fact is enhanced by the similar value of SDBP obtained for all the samples (Table 2). The low SDBP obtained for each individual tablet (mean value of 1.39%) indicated narrow spread of pixel values. In fact, there are two clear distributions. Most of the pixels had zero concentration of Lorazepam, which may indicate that the active principle was finely grounded and in a low concentration in the measured surface, but absent in the majority of the pixels. On the other hand, the pixels containing a certain amount of Lorazepam formed a Gaussian distribution with a mean value close to 2.5% (inlet of Fig. 4).

This clearly indicates that due to its low concentration, Lorazepam was not present in most of the pixels, which is not a contradiction with its fairly uniform distribution. The robustness and performance of the models were assessed by the low and randomly

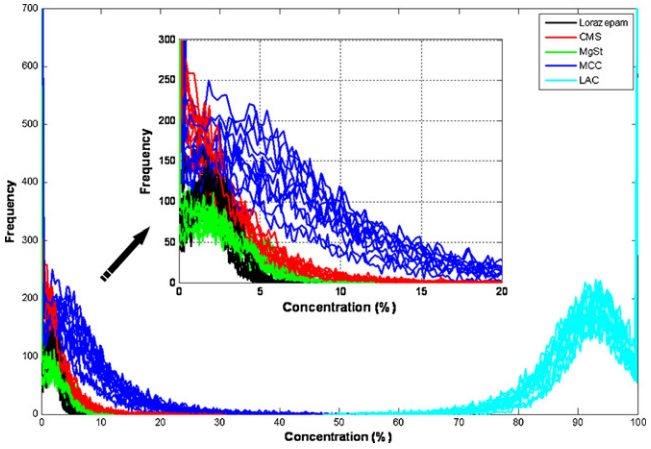

Fig. 4. Histogram plots for Lorazepam (black) and excipients (see legend).

distributed values around zero obtained in the residuals (results not shown). Moreover, the LOF percentages of the augmented MCR models for the 12 tablets was lower than 6%, denoting a correct development of the model and covering more than 99.64% of the total variance of each sample. It is worth stressing the high similarity (in terms of correlation coefficient) found between the spectral profiles obtained for Lorazepam with augmented MCR models and its pure spectrum (Table 1, Fig. 5). This is an important parameter to assess the performance of the models.

3.2. Distribution of the excipients

Spectral profiles calculated for the excipients were also in agreement with the corresponding pure spectra (Fig. 6). In general, they were highly correlated with the pure component spectrum (similarity coefficients higher than 0.999, Table 1).

Taking a deeper look to the figure of spectral profiles for LAC, an interesting deviation appears. This phenomenon may be explained

Table 2
SDBP values obtained for each sample and each compound.

	Lorazepam	CMS	MgSt	MCC	LAC
Sample 1	1.31	2.76	2.23	5.79	6.14
Sample 2	1.51	2.67	1.78	5.50	6.12
Sample 3	1.43	2.47	1.96	6.10	6.47
Sample 4	1.25	2.57	1.83	6.02	6.44
Sample 5	1.55	2.54	1.86	4.26	5.09
Sample 6	1.18	2.32	1.77	7.23	7.30
Sample 7	1.15	2.46	1.83	5.60	5.97
Sample 8	1.43	2.77	1.79	5.35	5.82
Sample 9	1.49	2.25	1.78	6.33	6.39
Sample 10	1.49	2.76	1.97	6.77	7.03
Sample 11	1.49	2.76	1.97	6.77	7.03
Sample 12	1.40	2.38	1.83	6.57	6.73
Mean[a]	1.39 ± 0.14	2.56 ± 0.19	1.88 ± 0.13	6.02 ± 0.80	6.38 ± 0.61
CV (%)[b]	9.77	7.29	6.96	13.29	9.58

[a] Mean value of the 12 samples and standard deviation (between brackets).
[b] Coefficient of variation calculated as $s * 100/\text{Mean}$.

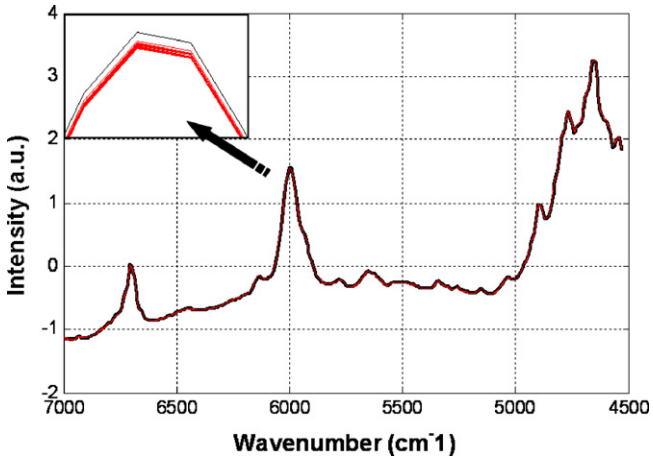

Fig. 5. Extracted spectral profiles for Lorazepam (red) from pre-processed data (SNV and smoothing) obtained with the augmented MCR model compared with the pure one (black). (For interpretation of the references to color in this figure legend, the reader is referred to the web version of the article.)

with the possible variation of the compression force in the manufacture of tablets or with the associated change in the particle size due to this variation. Since LAC was the compound found in higher concentrations (around 90%, see Table 1) it is plausible that any physical feature of the tablets may be reflected on it.

The concentration levels obtained for the excipients can be found in Table 1. As in the case of Lorazepam, the relative low standard deviation and variation coefficient denoted a correct repeatability between tablets. In addition, the shape of the histograms (Fig. 4) and the SDBP values (Table 2) were highly similar in all the samples.

The advantage of calculating the concentration maps for each compound in each tablet relies in the fact that further information about the distribution of each compound can be obtained. As an example, Fig. 7 depicts the concentration surfaces for the excipients of four of the twelve tablets studied.

As can be seen in Fig. 7, CMS forms small aggregates in all tablets, a normal display due to its hydrophilic properties. MgSt appeared in a more dispersive way (see tablet 1 in Fig. 7). In the images obtained for the first two tablets, a lower density is clearly observed in the top of the image than in the bottom, which is prone to yield inconsistency of the final tablet and, consequently, intake problems. The third excipient in importance was MCC. Despite being used as inactive filler, it should also be homogeneously distributed in the tablet to ensure the correct sharing of the rest of the active substances. However, it is possible to observe how MCC is forming some aggregates in not a very homogeneous distribution in several of the tablets analyzed (Fig. 7).

3.3. Quantitative surface distribution studies of Lorazepam and the excipients

As previously mentioned, the therapeutical dose in some cases may be a fraction of the commercial preparation. In those situations it is critical to prove that these physical fractions really contain the expected quantity of API.

This is a very complex problem that should be tackled in two steps. To simplify, only the case of tablets produced with a single score line will be considered. First of all, it is necessary to prove that tablets are indeed split into two equal halves, i.e. the mass of each fraction does not differ significantly from the half of the tablet mass. In a second step, it should be necessary to prove that both halves contain a similar amount of API.

Nowadays, regulatory authorities are only focused in the first step. For instance, the European Pharmacopoeia (01/2008:0478) only describes the procedure to demonstrate mass equality between halves. Several studies dealing with the subject have been published (van der Steen et al., 2010; van Santen et al., 2002). Moreover, the US-FDA has recently suggested some recommendations about tablet splitting

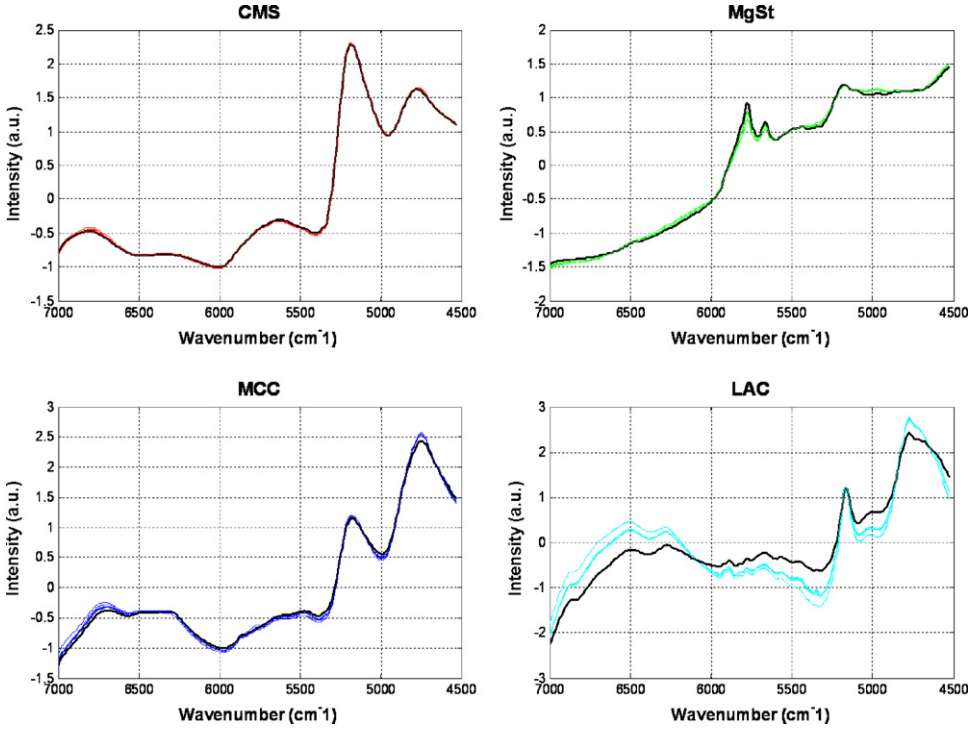

Fig. 6. Spectral profiles for the four excipients (in colors) from pre-processed data (SNV and smoothing) obtained with the augmented MCR model and comparison with the corresponding spectrum of the pure compound (black).

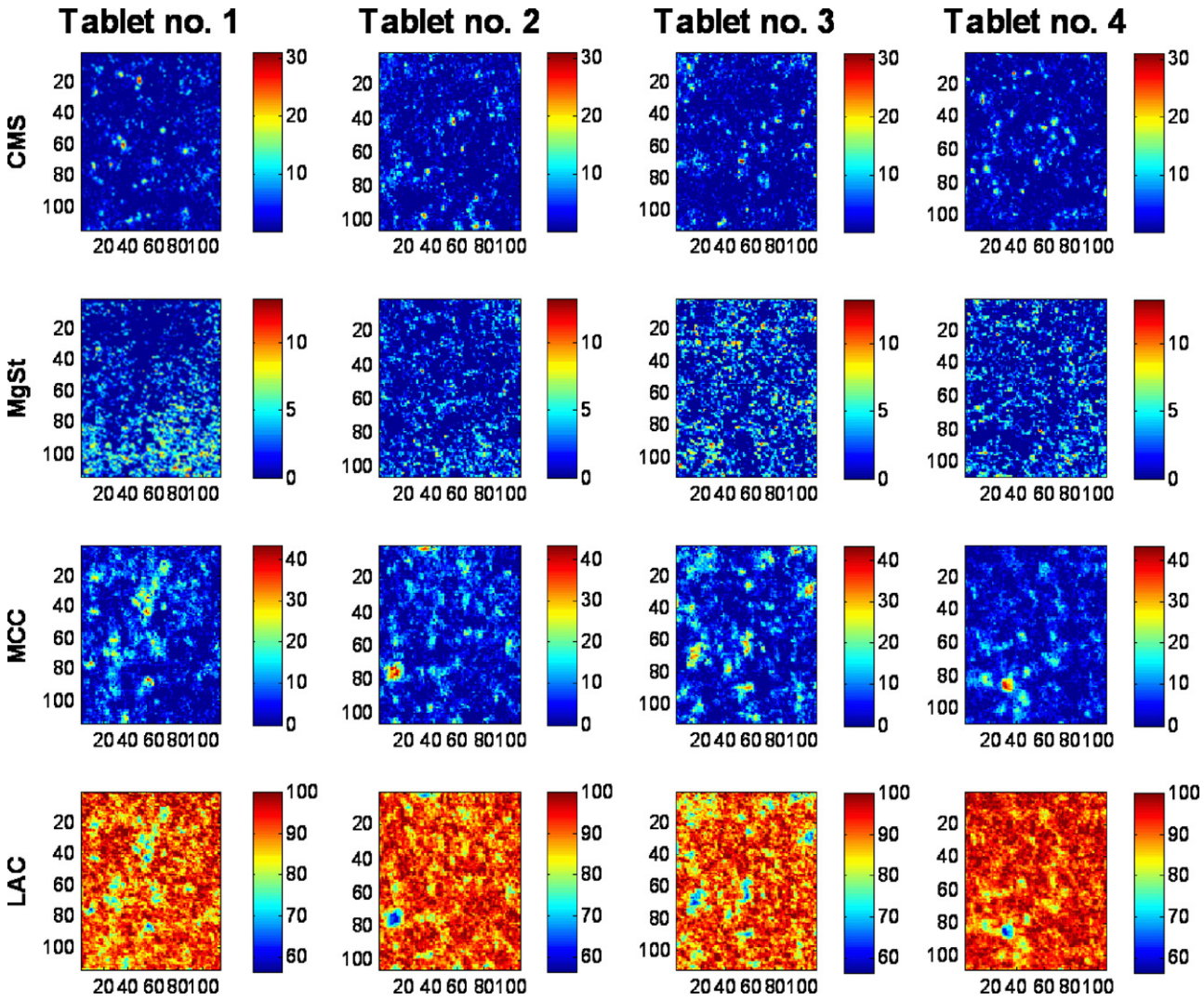

Fig. 7. Concentration maps for all the excipients in the first four tablets. Columns correspond to tablets and rows to the excipients (sodium carboxymethyl starch (CMS), magnesium stearate (MgSt), microcrystalline cellulose (MCC) and lactose monohydrate (LAC)). The color scale indicates the percentage of each component.

(www.fda.gov/AboutFDA/CentersOffices/CDER/ucm191353.htm, accessed December 2010).

Splitting the tablet is the most important practical issue. While for a major component it is a reasonable assumption that powder blending homogeneity has been achieved in the manufacturing process, the same is not so clear for APIs at a low concentration (e.g. around 1% mass fraction). In that context, CI has to be considered as a complementary technique, especially useful to tackle the second step in quality control of divisible tablets, that is, uniformity of content between tablet fractions. Despite the fact that the concentration maps estimated in the proposed work do not actually yield the exact mass distribution, it is clear that the results are consistent and can be used to determine the correct proportion of the total API in a given area. Nevertheless, the problem of stating significant differences when halves are considered arises. A practical and simple way to deal with it is to use the criterion established in the European Pharmacopoeia 2005 (01/2005:0478). This criterion establishes that for uniformity of content of single-dose preparations (Section 2.3.4), the preparation fails to comply with the test if more than one individual content is outside the limits (±15% of the nominal concentration for 10 tablets) or if one individual content is outside ±25% of the average content note (for 30 tablets).

As seen in Fig. 3, it is not always trivial to check the differences in distribution of a given compound in the tablet. The simple observation of the surface obtained by MCR cannot provide this information very accurately. For example, more than 55% of the Lorazepam content of tablet 7 (Fig. 8) is found on the right side of the tablet. In general, it is shown that Lorazepam is well distributed in the measured surface, with relatively low differences between the different parts of the tablet (all values are within ±15% of the limit).

However, higher differences can be found in the rest of the excipients (Fig. 8). Tablet 9, for instance, showed the highest differences in the distribution of CMS and MCC (Fig. 8a and c), close to a difference of 30% between halves. Particularly relevant is the distribution of MCC. It can be clearly observed that most of the content was in the top right part of the tablet (Fig. 8c). For MgSt distribution, the most heterogeneous distribution was found in the first tablet (Fig. 8b), clearly biased towards the bottom part of the surface. Only slight variability is expected for LAC, since it is the major compound in the tablets.

These differences in the surface distribution found for some of the tablets can be attributed to many facts. First of all, we have to be aware that this is a surface technique. Therefore, someone can argue that the scanned surface is not representative from the bulk sample. However, attending to the dimensions of the scanned surface (cross-sectioned surface from the tablet), the surface can be considered representative for the tablet. Apart from that, these differences could be attributed to some physical or

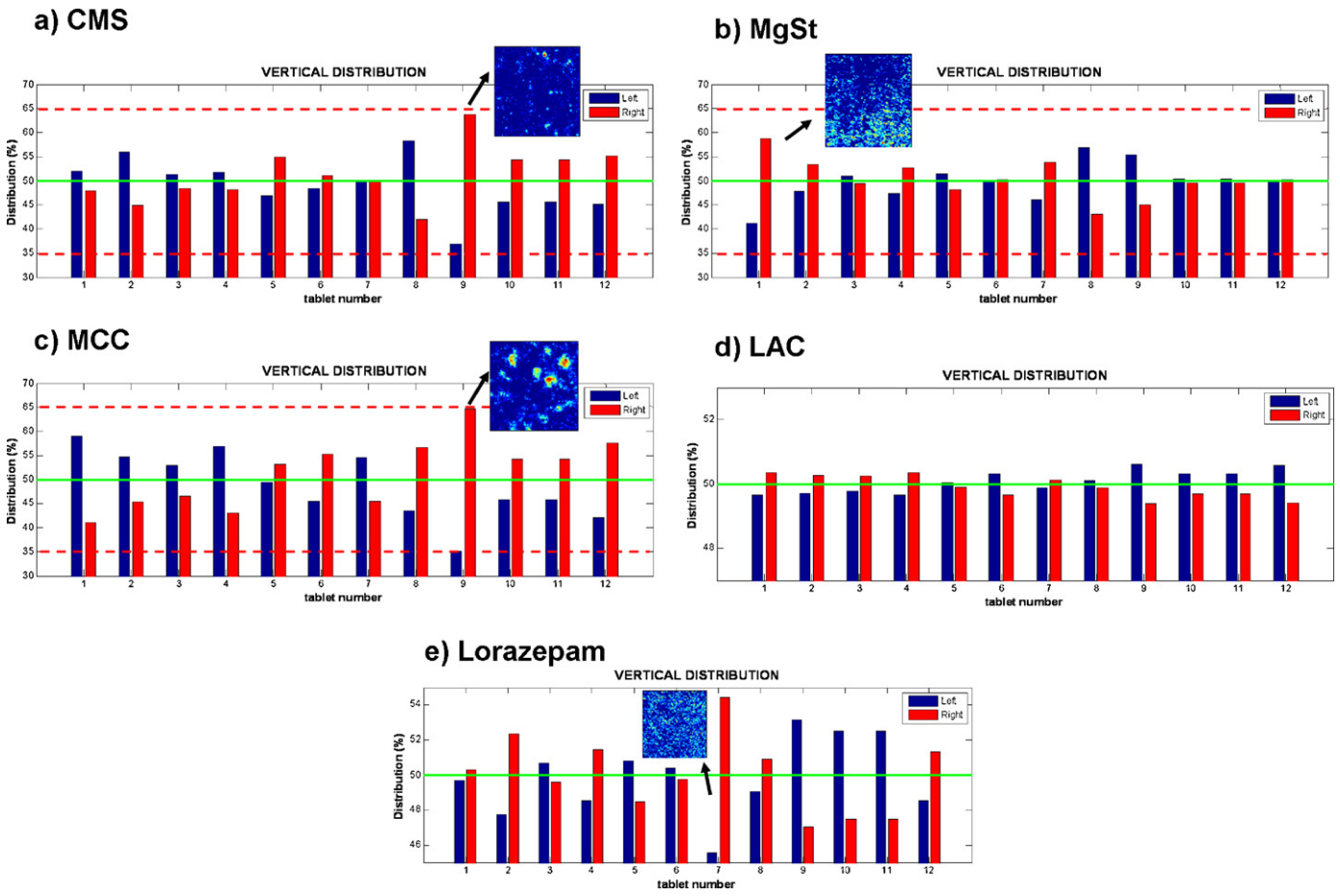

Fig. 8. Vertical distribution of excipients (a–d) and Lorazepam (e) in the tablets. The green line marks the theoretical nominal concentration in each half (50%). The dashed red lines mark the ±15% limit of the nominal concentration. (For interpretation of the references to color in this figure legend, the reader is referred to the web version of the article.)

chemical parameters (tabletting process, different compression forces between tablets, cohesive forces of the different excipients in the blending-granulation stages, etc.). What is important to highlight in this work is, precisely, the possibility of fast assessment of the surface distribution and, therefore, further possibility for troubleshooting.

4. Conclusions

The general conclusion of this work is that coupling NIR hyperspectral techniques with multivariate curve resolution methods is an adequate combination to study essential aspects in pharmaceutical tablets, namely the influence of each of its components and their distribution (homogeneity) in the studied surface.

Despite having only an approximate nominal bulk concentration of API in the tablet (≈1 wt%), it was possible to obtain a reliable estimation of the signal influence of all compounds in the Lorazepam tablets studied. Moreover, this signal influence value was close to the theoretical concentration (in percentage) of the compounds. The results found for the studied samples showed no significant variation between tablets. Also remarkable is the "physical" information obtained from lactose monohydrate spectral profiles, probably reflecting different compression forces in the manufacturing of commercial and standard tablets.

Once the concentrations maps have been obtained, it is easy to calculate the proportional distribution of API (or any other compound) in any desired fraction of the tablet, what can be a very useful complementary analytical procedure to the present pharmacopoeia regulations. This methodology can be easily adapted in the routinely analysis in the laboratory by merging the output of the hyperspectral device with the adequate software (MCR methodology in our case).

Acknowledging that the main limitation of hyperspectral techniques is that only information about the scanned surface is available, the proposed methodology may be an excellent opportunity to analyze the surface distribution of the different compounds of tablets routinely. Apart from the speediness of the analysis when compared to techniques like HPLC, crucial information can be obtained about the distribution of each compound. This allows the assessment of manufacturing process correctness, offering indirect information on the tablet intake behavior.

Acknowledgements

Dr. José Manuel Amigo strongly thanks Mrs. Rosa Rubio for her support in the development of this work. Felicidad Franch-Lage thanks Spanish Ministry for the fellowship (CTQ 2007-62528 project) and for her three-month stay in the Department of Food Science, Quality and Technology of the University of Copenhagen, Denmark.

References

E.C.E.a.I.D.-G.E., 2005. http://ec.europa.eu/enterprise/pharmaceuticals/eudralex/vol-2/c/spcguidrev1-oct2005.pdf (accessed December 2010).
Amigo, J.M., 2010a. Practical issues of hyperspectral imaging analysis of solid dosage forms. Anal. Bioanal. Chem. 398, 93–109.

Amigo, J.M., Ravn, C., 2009. Direct quantification and distribution assessment of major and minor components in pharmaceutical tablets by NIR-chemical imaging. Eur. J. Pharm. Sci. 37, 76–82.
Amigo, J.M., Cruz, J., Bautista, M., Maspoch, S., Coello, J., Blanco, M., 2008. Study of pharmaceutical samples by NIR chemical-image and multivariate analysis. Trends Anal. Chem. 27, 696–713.
Amigo, J.M., Ravn, C., Gallagher, N.B., Bro, R., 2009. A comparison of a common approach to partial least squares-discriminant analysis and classical least squares in hyperspectral imaging. Int. J. Pharm. 373, 179–182.
Aulton, M.E., 2007. Aulton's Pharmaceutics: The design and Manufacture of Medicines, 3rd ed. Elsevier, Churchill, Livingston.
Chan, K.L.A., Elkhider, N., Kazarian, S.G., 2005. Spectroscopic imaging of compacted pharmaceutical tablets. Chem. Eng. Res. Des. 83, 1303–1310.
Chen, D.T., Wynia, M.K., Moloney, R.M., Alexander, G.C., 2009. US physician knowledge of the FDA-approved indications and evidence base for commonly prescribed drugs: results of a national survey. Pharmacoepidemiol. Drug Safety 18, 1094–1100.
Cruz, J., Bautista, M., Amigo, J.M., Blanco, M., 2009. NIR-chemical imaging study of acetylsalicylic acid in commercial tablets. Talanta 80, 473–478.
de Juan, A., Tauler, R., 2006. Multivariate curve resolution (MCR) from 2000: progress in concepts and applications. Crit. Rev. Anal. Chem. 36, 163–176.
de Juan, A., Tauler, R., Dyson, R., Marcolli, C., Rault, M., Maeder, M., 2004. Spectroscopic imaging and chemometrics: a powerful combination for global and local sample analysis. Trends Anal. Chem. 23, 70–79.
de Juan, A., Maeder, M., Hancewicz, T., Duponchel, L., Tauler, R., 2009. Chemometric tools for image analysis. In: Salzer, R., Siesler, H.W. (Eds.), Infrared and Raman Spectroscopic Imaging. Wiley-VCH, pp. 65–112.
Furukawa, T., Sato, H., Shinzawa, H., Noda, I., Ochiai, S., 2007. Evaluation of homogeneity of binary blends of poly(3-hydroxybutyrate) and poly(L-lactic acid) studied by near infrared chemical imaging (NIRCI). Anal. Sci. 23, 871–876.
Gendrin, C., Roggo, Y., Collet, C., 2008. Pharmaceutical applications of vibrational chemical imaging and chemometrics: a review. J. Pharm. Biomed. Anal. 48, 533–553.
Jaumot, J., Gargallo, R., de Juan, A., Tauler, R., 2005. A graphical user-friendly interface for MCR-ALS: a new tool for multivariate curve resolution in MATLAB. Chemom. Intell. Lab. Syst. 76, 101–110.
Jovanovic, N., Gerich, A., Bouchard, A., Jiskoot, W., 2006. Near-infrared imaging for studying homogeneity of protein–sugar mixtures. Pharm. Res. 23, 2002–2013.
Lader, M., 1984. Short-term versus long-term benzodiazepine therapy. Curr. Med. Res. Opin. 8, 120–126.
Lewis, E.N., Carroll, J.D., Clarke, F.M., 2001. NIR imaging: a near infrared view of pharmaceutical formulation analysis. NIR News 12, 16.
Ravn, C. Near-Infrared Chemical Imaging in Formulation Development of Solid Dosage Forms. PhD Thesis. Department of Pharmaceutics and Analytical Chemistry. Faculty of Pharmaceutical Sciences. University of Copenhagen. Denmark, 2009.
Ravn, C., Bro, R., Skibsted, E., 2008. Near-infrared chemical imaging (NIR-CI) on pharmaceutical solid dosage forms—comparing common calibration approaches. J. Pharm. Biomed. Anal. 48, 554–561.
Reich, G., 2005. Near-infrared spectroscopy and imaging: basic principles and pharmaceutical applications. Adv. Drug Delivery Rev. 57, 1109–1143.
Roggo, Y., Edmond, A., Chalus, P., Ulmschneider, M., 2005. Infrared hyperspectral imaging for qualitative analysis of pharmaceutical solid forms. Anal. Chim. Acta 535, 79–87.
Rowe, R.C., Sheskey, P.J., Owen, S.C., 2006. Handbook of Pharmaceutical Excipients, fifth ed. Pharmaceutical Press and the American Pharmacists Association, London, p. 922.
van der Steen, K.C., Frijlink, H.W., Schipper, C.M.A., Barends, D.M., 2010. Prediction of the ease of subdivision of scored tablets from their physical parameters. AAPS PharmSciTech. 11, 126–132.
van Santen, E., Barends, D.M., Frijlink, H.W., 2002. Breaking of scored tablets: a review. Eur. J. Pharm. Biopharm. 53, 139–145.